The intra-seasonal variability of the convection in the Gulf of Guinea: *analysis of a 15-day mode of variability*

P. H. Kamsu Tamo[1,2], S. Janicot [1], D. Monkam[2], A. Lenouo[2]

[1]*Laboratoire d'Océanographie et du Climat: Expérimentation et Analyse Numérique/Institut Pierre Simon Laplace, Université Pierre et Marie Curie, Paris, France*

[2]*Université de Douala, Douala, Cameroun*

Context and Aim

Central Africa and Guinea gulf face rain during spring and fall.
Some intraseasonal variability signal has been highlighted during spring in the Guinea gulf (see talks in session 6A)
We have performed a general analysis of intraseasonal variability in spring based on a regional coastal index.
We have considered the role of convectively coupled Kelvin wave.

Data and methods

Data : Daily values over March-June (MAMJ) of :
- Rainfall from TRMM (1998-2010)
- OLR from NOAA's OLR (1979-2010)
- ERAI reanalysis of 925 hPa geopotential height and horizontal wind (1979-2010)

Methods :
- Analysis based on a regional index of OLR over the area of the maximum of variance (see Fig.1)
- Spectral analysis of the OLR index and 1-90-days filtering
- Regression of deseasonalised fields on the OLR index
- Wheeler-Kiladis spectral decomposition ; Kelvin-box filtering ; Guinean coastal Kelvin-filtered OLR index
- Singular spectrum analysis (SSA) of the 10-90 days filtered OLR index and of Kelvin-filtered index
- Regression of deseasonalised fields on the SSA OLR 10-90-day and Kelvin filtered indexes

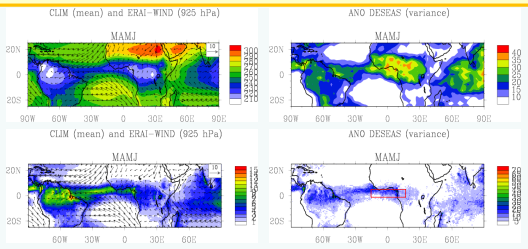

Fig.1: Left *Climatological mean of OLR (top) and Rain (bottom) over March-June 1998 to 2010. Arrows represent the 925 hPa horizontal wind.* ***Right*** *Associated variance. The red box delineated the region of the Guinean coast index from which our analyses are done.*

Variability in the Gulf of Guinea in spring

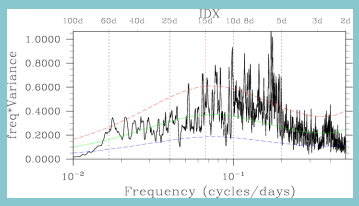

Fig.2*: MAMJ spectrum of the Guinea Coast index of 1-90 days filtered OLR*

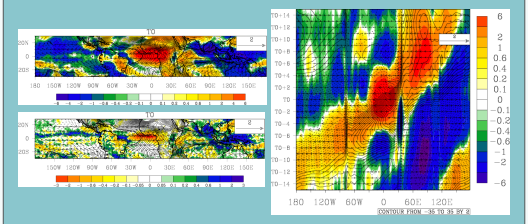

Fig.3 *: **Left top** Horizontal pattern at lag T0 of the regression coefficients between the OLR index and 1-90-day filtered OLR and 925hPa wind and geopotential. **Left bottom** Same as top but for rain. **Right:** Longitude-time diagram of the regression coefficients between the OLR index and unfiltered OLR (shaded), 925 hPa geopotential heigth (contour) and zonal wind (arrow) averaged over 5°N-5°S.*

What could be the role of the equatorial waves dynamics ?

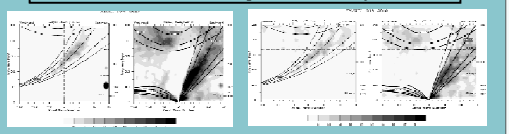

Fig.4 *NOAA-OLR **(Left)** and TRMM-rain **(Right)** (1979[1998]-2010 for OLR [rain]) wave number-frequency mean power spectrum over February-July and 15°N-15°S. Each panel presents the symmetric (right) and antisymmetric (left) component of the power spectrum plotted as the ratio between raw power and in the smoothed red noise background spectrum. The lines represented the dispersions curves delineating the mark of the convectively coupled equatorial waves (WK99).*

Kelvin wave variability in the Gulf of Guinea in spring

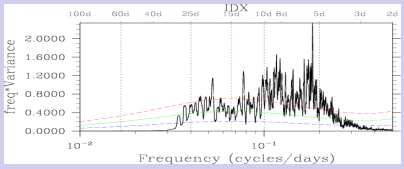

Fig.5*: MAMJ spectrum of the Guinea Coast index of Kelvin filtered OLR*

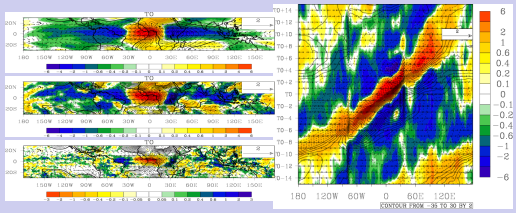

Fig.6 *: **Left top** Horizontal pattern at lag T0 of the regression coefficients between the Kelvin-filtered OLR index and : **top**: Kelvin filtered OLR (shaded), **middle:** deseasonalised OLR (shaded), **bottom**: unfiltered rain (shaded). **Right** Longitude-time diagram of the regression coefficients between the Kelvin-filtered OLR index and deseasonalised OLR. On each panel, the regression coefficients for the 925 hPa geopotential height (contour, dashed [full] lines represented the negatives [positives] values) and horizontal wind (arrows) have been plotted.*

Kelvin wave contribution to the intraseasonal variability in the Gulf of Guinea in spring

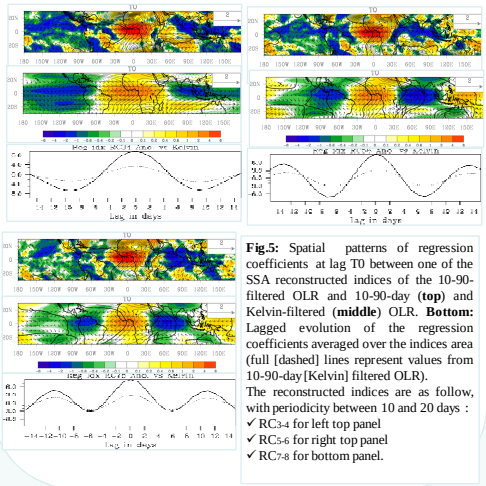

Fig.5: Spatial patterns of regression coefficients at lag T0 between one of the SSA reconstructed indices of the 10-90-filtered OLR and 10-90-day (**top**) and Kelvin-filtered (**middle**) OLR. **Bottom:** Lagged evolution of the regression coefficients averaged over the indices area (full [dashed] lines represent values from 10-90-day [Kelvin] filtered OLR).
The reconstructed indices are as follow, with periodicity between 10 and 20 days :
- ✓ $RC_{3\text{-}4}$ for left top panel
- ✓ $RC_{5\text{-}6}$ for right top panel
- ✓ $RC_{7\text{-}8}$ for bottom panel.

SSA decomposition of the 10-90-filtered and the Kelvin-filtered OLR indexes

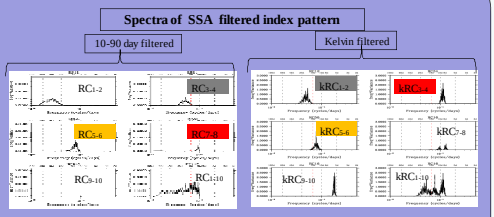

Fig.4: *Spectra of the reconstructions of the filtered OLR indexes by pairs of SSA components. Coloured boxes show up SSA reconstructions with similar spectra. The related three reconstructed indices are used in regression of 10-90-day (left) and Kelvin (right) filtered OLR at lag T0 below.*

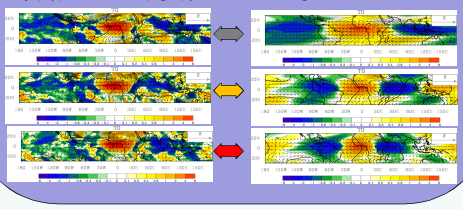

Tab.1: Dominant periods and explained variance (%) associated to the five first modes revealed by the SSA applied to 10-90-day filtered OLR

Mode	Periods (days)	Expl. Var. (%)
1 (RC12)	25.0 – 90.0	35.7
2 (RC34)	15.0 – 20.0	25.8
3 (RC56)	11.1 – 16.0	23.0
4 (RC78)	10.0 – 12.5	11.8
	Total	96.3

Tab.2: Dominant periods and explained variance (%) associated to the five first modes revealed by the SSA applied to Kelvin-filtered OLR

Mode	Periods (days)	Wavelength (km)	Phase speed (m/s)	Expl. Var (%)
1 (kRC12)	15.0 – 30.0	~27800	~16.09	18.8
2 (kRC34)	8.0 – 11.0	~13400	~18.0	15.7
3 (kRC56)	10.0 – 16.0	~16200	~13.3	13.0
4 (kRC78)	-	-	-	12.0
5 (kRC910)	~6.0	~6.0	-	10.3

This study is based on a regional index along the Guinean Coast where the variance is the highest (domain [2°S-5°N; 20°W-10°E]). This index has been used to regressed deseasonalised and Kelvin filtered OLR, rain and 925hPa geopotential and wind data.

Fig.2 shows that intraseasonal signals and synoptic ones are significant along the Guinean Coast in spring. It is also shown on **Fig.3** that this variability is associated with a mean eastward propagation of both convective and atmospheric patterns. Moreover the horizontal structure of fields at lag T0 is similar to a Kelvin wave structure. So we focus on the contribution of the Kelvin wave dynamics.

We applied the SSA decomposition on both 10-90-day and Kelvin filtered OLR indices (**Fig.4**). This enables to extract independent modes with a specific periodicity. **Tab.1** and **Tab.2** show the periods and explained variances of these modes. Also showed the phase speed of the corresponding waves. Three modes have been retained, whose dominant periodicities belong between 10 and 20 days, with a similar spectrum for 10-90-day and Kelvin filtered signal. Their associated regression patterns look similar too (**Fig.4**).

Fig.5 shows the respective 10-90-day and Kelvin filtered patterns for each of these three modes as well as the time-lagged series of the averaged regression coefficients over the Guinean Coast domain. For each of these modes the contribution of the Kelvin signal is significant both on the spatial pattern and on its amplitude.

Conclusion & perspectives

We have shown that Kelvin waves have a significant contribution on the intraseasonal variability (periodicities around 15 days, and phase speed from 13 to 18 m/s) of convection and rain along the Guinean Coast during spring.

In the following, we will evaluate on case studies the skill of regional modeling to reproduce these Kelvin waves, and their predictability.